Analysis of the Impact of Microgrid Penetration on Power System Dynamics

P. Ferraro, *Student Member, IEEE*, E. Crisostomi, *Member, IEEE*, M. Raugi, and F. Milano, *Fellow, IEEE*

Abstract— The paper proposes a stochastic model to analyse the dynamic coupling of the transmission system, the electricity market and microgrids. The focus is on the impact of microgrids on the transient response of the system and, in particular, on frequency variations. Extensive Monte Carlo simulations are performed on the IEEE 39-bus system, and show that the dynamic response of the transmission system is affected in a non trivial way by both the number and the size of the microgrids.

Index Terms— Microgrid, electricity market, distributed energy resources, transient stability analysis, frequency control.

I. INTRODUCTION

A. Motivation

In recent years, the advent of power system deregulation and the drift from a vertically integrated utility business model substantially changed the development of power industry and technology. The very protagonist of this new paradigm is the so called *smart grid* [1]. In this context, the concept of microgrid (MG) has received particular attention from the scientific community as it is generally considered the building block of the smart grid [2]. The MG can be defined as an electrical entity that facilitates a high depth penetration of DERs and relies on advanced control strategies. A less abstract definition is provided by the U.S. Department of Energy: *A MG is a group of interconnected loads and DERs with clearly defined electrical boundaries that acts as a single controllable entity with respect to the grid and can connect and disconnect from the grid to enable it to operate in both grid-connected or island mode* [3].

This new paradigm combined with the recent trend of the energy market deregulation, that will allow a MG to apply new policies of Demand & Response, is expected to bring economic advantages to the users and to increase the efficiency of the power grid as a whole. Nevertheless, the electrical system nowadays still heavily relies on centralized generation from traditional rotating machines. It is highly unlikely that a transition to a fully distributed transmission system will happen in the near future. Furthermore, due to the MGs ability to conduct policies of Demand & Response, a reliable and secure penetration of these units might prove to be a challenge to attain [4]. For this reason, it appears useful and timely

Pietro Ferraro, Emanuele Crisostomi and Marco Raugi are with the Department of Energy, Systems, Territory and Constructions Engineering, University of Pisa, Italy. (e-mails: pietro.ferraro@unipi.it, emanuele.crisostomi@unipi.it, marco.raugi@unipi.it).

Federico Milano is with the School of Electrical and Electronic Engineering of the University College Dublin, Belfield, Ireland. (e-mail: federico.milano@ucd.ie).

to study the behavior of the power system dynamics as a significant number of MGs is plugged into the transmission system and interacts with the electrical market.

B. Literature Review

While there has been a considerable amount of research carried out on the control of single, often islanded, MGs and on the investigation of the penetration level of DERs, the literature on the interaction between MGs, the market and its effect on the grid is limited. A relevant review on the impact of low rotational inertia in the power system frequency has been presented in [5]. In [6], angle and voltage stability is analysed as the MG penetration level increases and, in [7] and [8], the influence of high penetration of wind based DERs is assessed. In the aforementioned works, the ability of a MG to conduct policies of Demand & Response and its effect on the frequency control of the transmission system is not taken into consideration. Frequency deviations, in fact, are a measure of the active power imbalance and should remain within the operational limits in order to avoid transmission line overloads and the triggering of protection devices [9].

It is the authors' opinion that the MGs interaction with the electricity market is a crucial element that can not be neglected: a MG adopts a greedy behavior with respect to the electrical grid, selling or buying energy whenever it is convenient from an economical and operational point of view not necessarily taking into consideration the effects on the stability of the system. This behavior is acceptable only if the penetration of MGs is small with respect to the total system capacity and, due to their small size, MGs can be reasonably modeled as price takers. This situation, however, might not be acceptable if such a penetration increases.

Examples of works that take into account both MGs and the electricity market are [12] and [13]. In these works, however, the effect of the MG penetration level on the transient response of the power system are not investigated. On the other hand, a study on how an equivalent dynamic model of the electricity market impacts on power system transients is studied in [10]. The paper highlights potential instabilities that arise when the dynamics of the machines and of the loads are coupled with the dynamics of the energy market. In [11] the model developed in [10] is generalized by taking into account the effects of time delays and market clearing time on the stability of the system.

C. Contributions

To the best of the authors' knowledge, the effects on the power grid of greedy MGs has not been properly studied yet. This paper aims at filling this gap by merging together the electricity market model proposed in [10] with a hybrid dynamic and event-driven MG representation as well as a detailed electromechanical model of the system. The goal is to provide a dynamic model to study the coupling between the dynamics of the MGs, the power system and the electrical market, with an emphasis on frequency regulation. In particular, the paper provides the following contributions with respect to the state of art.

- An analysis of the dynamic impact of an increasing penetration level of MGs on power systems, coupled with market dynamics.
- A realistic time-domain analysis of the power system that takes into account detailed non linear electro-mechanical models, MGs, storage units and DERs.
- An analysis of the effects of different storage capacity sizes and different granularity of MGs on the stability of the power system.

D. Organization

The remainder of the paper is organized as follows. Section II describes the dynamic model employed. Section III presents a case study based on the IEEE 39-bus system. In the case study, the penetration level, the correlation, and the granularity of the MGs is duly evaluated through a Monte Carlo method and stochastic time domain simulations. Main conclusions and future work are outlined in Section IV.

II. MODELING

An MG is, at its core, a cluster of loads and generation units, coordinated by an Energy Management System (EMS) that, among other tasks (e.g., load shedding and internal power flow management), allows the MG to operate in island mode (i.e., the MG operates autonomously from the power grid) and determines the set point of the active power that the MG sells or buys from the electrical grid [16].

The objective of this work is to determine the impact of the penetration level, correlation and granularity of MGs on the dynamic response of the transmission system of the power grid. With this aim, the following assumptions appear sensible.

- The dynamics of the MG internal generation units and loads are neglected. This is not a strong assumption as the time constants of the internal MG dynamics are small compared to the ones of the high voltage transmission system [14], [15], [17].
- The storage units, the DERs and the loads of each MG are grouped into an aggregated model. This assumption allows reducing the computational burden of the proposed MG model.
- Due to their relatively small capacity, MGs are assumed to be price takers. Moreover, MG active power set-points depend on the electricity price. This assumption is consistent with the MG paradigm usually considered in the literature [3].

The remainder of this section describes the power system as well as the electricity market models considered in the simulations. Then, the proposed hybrid dynamic and event-driven MG model is discussed in detail.

A. Power grid simulations

Let us recall first conventional Differential Algebraic Equation (DAE) models, described by the following equations:

$$\dot{x} = f(x, y, u) \tag{1}$$
$$0 = g(x, y, u)$$

where f ($f : \mathbb{R}^{p+q+s} \mapsto \mathbb{R}^p$) are the differential equations; g ($g : \mathbb{R}^{p+q+s} \mapsto \mathbb{R}^q$) are the algebraic equations; x ($x \in \mathbb{R}^p$) are the state variables; y ($y \in \mathbb{R}^q$) are the algebraic variables; and u ($u \in \mathbb{R}^s$) are discrete events, which mostly model MG EMS logic.

The set of equations in (1) includes lumped models of the transmission system and conventional dynamic models of synchronous machines (e.g., 6th order models) and their controllers, such as, automatic voltage regulators, turbine governors, and power system stabilizers, as well as DERs, storage devices and the controllers included in the MGs, which are duly described in Subsection II-C.

B. Electricity Market Model

The power system model discussed in the previous subsection is assumed to be coupled with a real-time – or *spot* – electricity market model. This model represents a market for which the price, which is considered a continuous state variable, is computed and adjusted rapidly enough with respect to the dynamic response of the transmission system (e.g., PJM, California, etc.) [10]. Note that, while real-time markets are not particularly common at this time, the fast response of electricity price is expected to become a crucial and fundamental feature of future power systems with large penetration of renewable energy sources and MGs [18].

The model of market dynamics considered in this paper follows closely the work by Alvarado *et al.* [10]. The main assumption of such a model is that price variations are driven by the energy imbalance in the grid. An excess of supply decreases the price of energy while an excess of demand increases it. The following equations describe an ideal market with a single price of energy and with n power suppliers and m power consumers:

$$\dot{E} = \sum_{i=1}^{n} P_{Gi} - \sum_{j=1}^{m} P_{Dj} - P_{\text{loss}} \tag{2}$$

$$T_\lambda \dot{\lambda} = -K_E E - \lambda \tag{3}$$

where P_{Gi} are the generated active powers of the n suppliers connected to the grid; P_{Dj} are the active power consumption of m loads connected to the grid; P_{loss} are the active power losses in the transmission system; E and λ, are the energy imbalance and the electricity price, respectively; and K_E and T_λ are parameters that depend on the design of the market itself. Since in real-world systems it is hard to measure the power imbalance in (2), such an imbalance is deduced in [10]
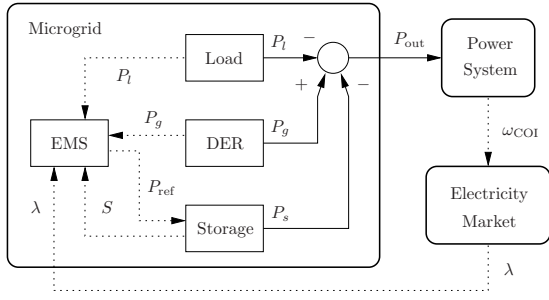
Fig. 1: Structure of the connection between the MG.

Fig. 2: Control scheme of an converter-based DER. The blocks show a first order dynamics expressed in the Laplace domain.

implicitly based on the frequency deviation of the center of inertia (COI). Hence, (3) the market clearing price dynamic is expressed as

$$T_\lambda \dot{\lambda} = K_E(1 - \omega_{\text{COI}}) - \lambda \qquad (4)$$

where ω_{COI} is the frequency of the COI, defined as

$$\omega_{COI} = \frac{\sum_{i=1}^{r} H_i \omega_i}{\sum_{i=1}^{r} H_i} \qquad (5)$$

where ω_i and H_i are, respectively, the frequency and the moment of inertia of the i-th synchronous machine, and r is the number of conventional generators in the grid.[1]

Finally, generator and load active powers are linked to the market clearing price λ based on a dynamic version of their bidding functions, as follows [10]:

$$T_{Gi}\dot{P}_{Gi} = \lambda - c_{Gi}P_{Gi} - b_{Gi} \qquad (6)$$
$$T_{Di}\dot{P}_{Di} = -\lambda - c_{Di}P_{Di} - b_{Di}$$

where, c_{Gi}, c_{Di} and b_{Gi}, b_{Di} are proportional and fixed bid coefficients, respectively, as in conventional auction models and T_{Gi} and T_{Di} are time constants modeling generator and demand, respectively, delayed response to variations of the market clearing price λ. Note that in [10] the equations for the load active powers are expressed with different signs. In this paper, all coefficients are assumed to be positive.

C. Microgrid Model

Figure 1 shows the overall connection of the MG with the power system and the electricity market. The elements that compose the microgrid are the load, the DER, the storage device and the energy management system (EMS) that collects the information of consumed and generated powers by other elements of the microgrid, the state of charge of the storage device, the electricity price λ and imposes the reference power generation P_{ref}.

The dynamic of the aggregated storage device model is ruled by the following equation, which is the time-continuous equivalent of the model used in [12],

$$T_c\dot{S} = P_s$$
$$= P_g - P_l - P_{\text{out}} \qquad (7)$$

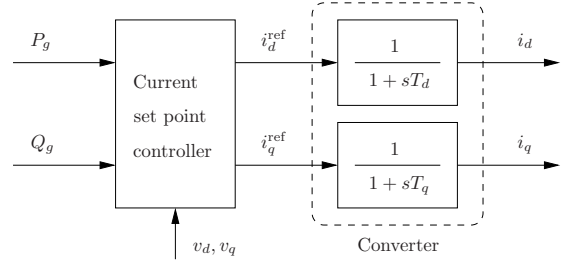[1]Note that, in general, $n \neq r$ as not all power plants are equipped with synchronous machines.

where S is the state of charge of the MG, T_c is the time constant of the state of charge of the storage unit, P_s is the power generated or absorbed by the storage device ($P_s > 0$ if the storage is charging); P_{out} is the power output of the MG; and P_g and P_l are the produced active power and the local loads, respectively, of the MG. S undergoes saturation hard-limits that model the fully charged and discharged conditions.

The DER dynamic model included in the microgrid is an elaboration of the DER models discussed in [19], [20]. The control scheme included in the DER model is shown in Fig. 2. This model is suitable for transient and voltage stability analysis and, hence, only current controllers of the VSC included in the DER are modeled. Power injections into the AC bus are:

$$P_g = v_d i_d + v_q i_q \qquad (8)$$
$$Q_g = v_q i_d - v_d i_q$$

where i_d and i_q are the AC-side dq-frame currents of the VSC, respectively and v_d and v_q are the dq-frame components of the bus voltage phasor of the point of connection of the VSC with the AC grid. The reference currents i_d^{ref} and i_q^{ref} are obtained from active and reactive powers P_g and Q_g, as follows:

$$\begin{bmatrix} i_d^{\text{ref}} \\ i_q^{\text{ref}} \end{bmatrix} = \begin{bmatrix} v_d & v_q \\ v_q & -v_d \end{bmatrix}^{-1} \begin{bmatrix} P_g \\ Q_g \end{bmatrix} \qquad (9)$$

Both i_d^{ref} and i_q^{ref} are bounded by the converter thermal limits.

Uncertainty and volatility of both generation units and loads are accounted for by modeling the net power produced by the MG as a stochastic process according to

$$P_{\text{net}} = P_g - P_l \qquad (10)$$
$$= \bar{P}_{g_T} - \bar{P}_{l_T} + \eta_M$$

where η_M has a stochastic process as in [21] with standard deviation σ_M, and $\bar{P}_{g_T}$ and $\bar{P}_{l_T}$ are piece-wise constant functions that account for uncertainty and change randomly with a period T as discussed in [22]. The noise is modeled as a single stochastic state variable as the behavior of the MG depends on the difference $P_{\text{net}} = P_g - P_l$ and not on their absolute value. For illustration, Fig. 3 shows 1,200 seconds of a realization of such a process, in which T is set to 300 seconds.

The EMS is based on a set of *if-then* rules to decide the most convenient active power set point, P_{ref}. In the simulations we assume that P_s, e.g., the power produced or absorbed by
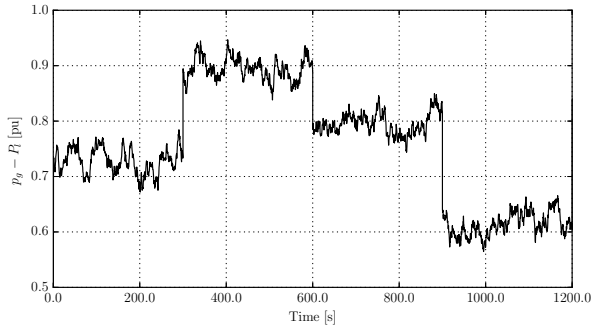
Fig. 3: Realization of the process used to simulate the behavior of the generation and the loads of a MG. The time interval after which the value changes is 300 seconds.

the aggregated storage device included in the MG is the slack variable that allows imposing the desired P_{ref}, as follows:

$$T_s \dot{P}_s = P_{\text{out}} - P_{\text{ref}}$$
$$= -P_s + P_{\text{net}} - P_{\text{ref}} \tag{11}$$

where T_s is the time constant of the storage active power controller.

EMS input quantities are the produced power P_g, the load P_l, the price λ and the state of charge of the storage units, S. The rules are divided into two sets: the seller state, for which $P_{\text{net}} \geq 0$ (i.e., the MG is producing more than it is consuming and it will most likely sell energy) and the buyer state, for which $P_{\text{net}} < 0$ (i.e., the MG is consuming more than it is producing and it will most likely buy energy). EMS parameters, ϵ_l, ϵ_h, k_s, k_b, P_{buy}, K_{buy}, P_{ch}, K_{ch} are specific of each MG, i.e., they depend on the market strategy of the MG owner or on its marginal cost (all the EMS parameters are positive). The meaning and purpose of these parameters is given in Table I. In particular, ϵ_l and ϵ_h indicate two thresholds under and above which the price of energy is considered, low and high, respectively. These thresholds are time-varying as the *convenience* of buying and selling energy depends on the current energy price. For example, if, in given period, the electricity price is around a value $\bar{\lambda}_1$, and the next period is around $\bar{\lambda}_2$, then one can set $\epsilon_{l1} \neq \epsilon_{l2}$ and $\epsilon_{h1} \neq \epsilon_{h2}$ to reflect the variation of market conditions. In the following, ϵ_l and ϵ_h are calculated as:

$$\epsilon_h = (1 + \rho)\bar{\lambda} \tag{12}$$
$$\epsilon_l = (1 - \rho)\bar{\lambda}$$

where $\bar{\lambda}$ is the average value of the price and ρ is a threshold that accounts for the fluctuation of the price in a given period. In the simulations discussed in Section III, it is assumed that $\rho = 0.0025$.

The aforementioned rules are listed and explained in Table I. The rules are expressed hierarchically; this means that a rule is evaluated only if the conditions on the previous ones are not satisfied. Note that, even if the MG production is greater than its consumption, the EMS can, in some cases, impose to buy energy, e.g., if the storage is empty and the electricity price is low. Similarly, even if the MG production is lower than its

consumption, the EMS can impose to sell energy if the storage is full and the price is high.

The EMS rules utilized in this paper are only a possible choice. There are several proposed EMS schemes in the literature – see, for example, recent works [23]–[27] and references therein. A comparison of different MG management schemes, however, is beyond of the scope of this paper.

III. CASE STUDY

As anticipated in the previous section, the active power set points of the MGs depend, among other variables, on the electricity price. This feature is the main difference between a MG and a DER unit: while a renewable resource usually injects into the grid all available power – which often evolves according to a stochastic process – a MG adopts a greedy behavior with respect to the electrical grid. In fact, the EMS will sell or buy energy when it is convenient from an economical and operational point of view, while in other cases it will store the surplus of produced energy in its storage units, thus effectively islanding the MG from the power grid, i.e., $P_{\text{out}} = 0$.

This case study discusses whether a high penetration of MGs within the electrical grid, without a proper coordinated control, is sustainable for the power system. In particular, the case study is aimed at defining the impact of the MG penetration level, correlation and granularity, and of the storage capacity on the frequency of the COI. Four scenarios are considered, as follows.

a) *Microgrid Scenario.* An increasing number of large MGs is plugged into the system.
b) *DER & Microgrid Scenario.* A mix of DERs and MGs is plugged into the system.
c) *High Granularity Microgrid Scenario.* The MGs of the first scenario are split into several smaller MGs.
d) *Large Capacity Storage Microgrid Scenario.* An increasing number of MGs, with large storage capacity devices, is plugged into the system.

Simulations are based on the IEEE 39-bus 10-machine system; this benchmark grid is chosen in order to have both a fairly complex network and reduced state-space dimensions to easily understand the impact of MGs on the system. The state-space of the simplest case with 1 MG includes 150 state variables and 233 algebraic ones; whereas the case with highest granularity includes 108 MGs, 685 state variables and 1,421 algebraic ones. The results for each scenario are obtained based on a Monte Carlo method (500 simulations are solved for each scenario), in order to account for a large number of stochastic strong trajectories and, hence, accurately infer statistical properties. Accordingly, the standard deviation of the frequency of the COI, σ_{COI}, is computed as the average of the standard deviation obtained for each realization.

All simulations are obtained using Dome, a Python-based power system software tool [28]. The Dome version utilized in this case study is based on Python 3.4.1; ATLAS 3.10.1 for dense vector and matrix operations; CVXOPT 1.1.8 for sparse matrix operations; and KLU 1.3.2 for sparse matrix factorization. All simulations were executed on a server mounting 40 CPUs and running a 64-bit Linux OS.

TABLE I: Microgrid EMS rules

Seller mode, $P_{\text{net}} \geq 0$

Rule	Action	Rationale
if $S \geq 80\%$ and $\lambda \geq \epsilon_h$	$P_{\text{ref}} = P_{\text{net}}(1 + k_s)$	The price of energy is high and the battery is fully charged. It is convenient to sell more energy
else if $S \geq 80\%$ or ($50\% \leq S < 80\%$ and $\lambda \geq \epsilon_h$)	$P_{\text{ref}} = P_{\text{net}}$	Sell the surplus
else if $\epsilon_l \leq \lambda < \epsilon_h$ or ($50\% \leq S < 80\%$ and $\lambda < \epsilon_l$)	$P_{\text{ref}} = 0$	Charge the storage with the production surplus
else if $\lambda < \epsilon_l$ and $S < 50\%$	$P_{\text{ref}} = -P_{\text{buy}} - K_{\text{buy}}\lambda$	Storage is low on charge and, despite the surplus of production, it is convenient to buy energy proportionally to the price (i.e., the lower the price the more the EMS can buy)

Buyer mode, $P_{\text{net}} < 0$

Rule	Action	Rationale
if $S \leq 20\%$	$P_{\text{ref}} = P_{\text{net}} - P_{\text{ch}}$	Storage is very low on charge, buy the deficit of energy plus an extra amount to charge the storage
else if $\lambda \geq \epsilon_h$ and $S \geq 80\%$	$P_{\text{ref}} = P_{\text{net}}(1 + k_b)$	The price of energy is very high and the storage is full, sell energy
else if $\lambda \geq \epsilon_h$ and $50\% \leq S < 80\%$	$P_{\text{ref}} = 0$	The price of energy is very high and the storage has a medium charge, use it to compensate the energy deficit
else if $\lambda \geq \epsilon_h$ and $S < 50\%$	$P_{\text{ref}} = P_{\text{net}}$	The price of energy is high and the storage is medium-low on charge, buy the energy deficit
else if $\lambda \leq \epsilon_l$ and $S < 80\%$	$P_{\text{ref}} = P_{\text{net}} - P_{\text{ch}} - K_{\text{ch}}\lambda$	The price of energy is very low and the storage is not fully charged, buy an extra amount of energy to store, proportional to the price (i.e., the lower the price the more the EMS can buy)
else if $\lambda \leq \epsilon_l$ and $S \geq 80\%$	$P_{\text{ref}} = P_{\text{net}}$	The price of energy is very low and the storage is fully charged, buy the energy deficit
else if $\lambda > \epsilon_l$ and $S \geq 50\%$	$P_{\text{ref}} = 0$	The price of energy is not very low and the storage are is medium-high on charge, use it to compensate the energy deficit
else if $\lambda > \epsilon_l$ and $20\% < S < 50\%$	$P_{\text{ref}} = P_{\text{net}}$	The price of energy is not very low and the storage is medium-low on charge, buy the energy deficit

A. Microgrid Scenario

This scenario consists in studying the impact on the grid of an increasing number of large MGs. Note that the MGs are not assumed to be large *per se*. Rather, they model large aggregated networks of MGs whose power generation, consumption and EMSs are assumed to be either centrally coordinated or strongly correlated. Table II shows the parameters for the considered MGs while Fig. 4 shows all the realizations of the frequency of the COI, ω_{COI}, for 2, 6 and 12 MGs. In Table II, $\bar{P}_g$ and $\bar{P}_l$ indicate average values of P_g and P_l, respectively, during the simulation, while σ_{net} is the standard deviation of the net active power production P_{net}. In the four cases, the MG capacity and the average ratio between the active power provided by the MGs and the active power provided by conventional power plants are, respectively, 1.81, 3.13, 4.52 and 5.84 (pu MW); and 2.1%, 3.8%, 1.44% and 2.4%. The ratio does not increase with the number of MGs because each unit is able to buy or sell power from the grid (i.e., some of the units are, on average, loads). It is clear, even from visual inspection, that the standard deviation of ω_{COI} increases as the number of units plugged into the system gets higher, increasing, approximately, from 0.0005 to 0.0018. In particular, Table III shows the σ_{COI}, as a function of the number of MGs, ranging from 1 to 12. This result is consistent with the size of each MG and their reduced number. The increasing number of MGs, in fact, leads the variations of P_{net}

TABLE II: Microgrid parameters

MG	Bus	$\bar{P}_g$ (pu MW)	$\bar{P}_l$ (pu MW)	T_c (s)	σ_{net} (pu MW)
1	18	0.88	0.54	5.0	0.025
2	3	0.77	0.20	7.0	0.040
3	15	0.80	0.10	6.5	0.030
4	17	0.40	0.20	8.0	0.020
5	21	0.20	0.10	5.0	0.013
6	28	0.20	0.40	7.0	0.040
7	24	0.36	0.84	6.5	0.010
8	17	0.20	0.50	8.0	0.020
9	11	0.20	0.30	9.0	0.010
10	5	0.10	0.80	5.0	0.010
11	7	0.80	0.10	7.4	0.030
12	12	0.40	0.40	6.8	0.025

to increase, which directly impact on the standard deviation of ω_{COI}.

Figure 5 shows the fluctuations of the market clearing price λ for the cases with 2, 6 and 12 MGs. Note that both the mean value and the amplitude of the variations of λ are affected by the number of MGs included into the system. The fact that the market clearing price volatility increases as the number of MG increases is a consequence of λ being dependent on ω_{COI}, according to (4). Furthermore, the more λ fluctuates, the more frequently each MG adjusts its active power set-point P_{ref}, thus increasing the fluctuations of ω_{COI}.

Fig. 6 shows the trajectories of the power outputs of three

TABLE III: Standard deviation of the frequency COI as a function of the total MG installed capacity

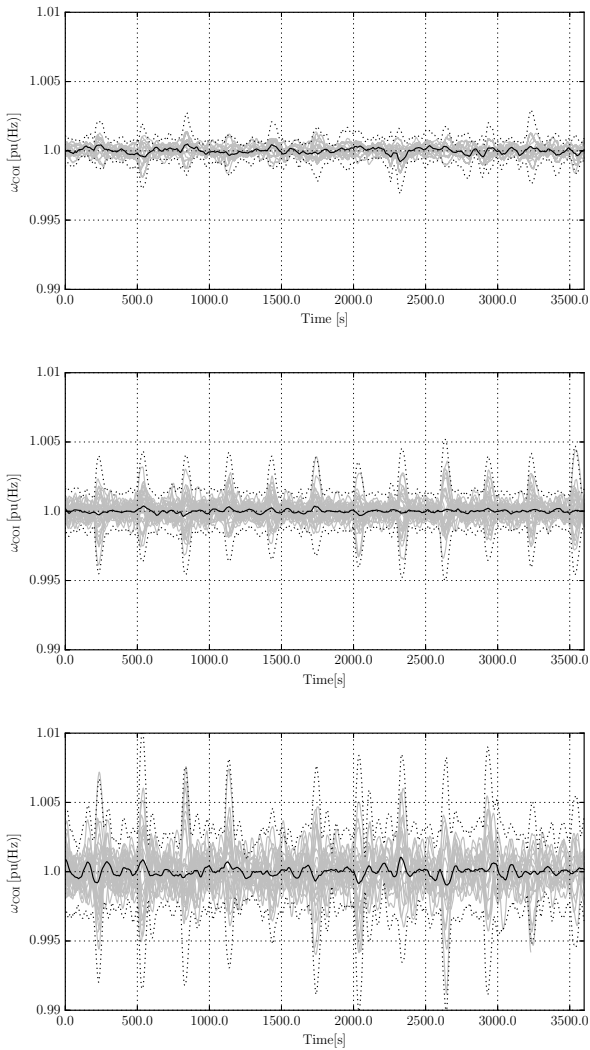| MG	Capacity (pu MW)	σ_{COI} (pu Hz)
1	0.96	0.000276
2	1.81	0.000514
3	2.69	0.000584
4	3.13	0.000893
5	3.35	0.000934
6	3.57	0.001121
7	3.97	0.001247
8	4.19	0.001352
9	4.41	0.001401
10	4.52	0.001407
11	5.40	0.001602
12	5.84	0.001788

Fig. 4: Frequency ω_{COI} with 2 (upper panel); 6 (middle panel); and 12 (lower panel) MGs. The grey lines represent each realization, the black thick line represents the average of the process, while the dotted line represents the average ± 3 times the standard deviation.

MGs for one realization of the case with 12 MGs. As it can be observed, depending on the set points and parameters, an MG can be always in buyer (MG 6) or seller (MG 5) mode or can alternate between the two modes (MG 10).
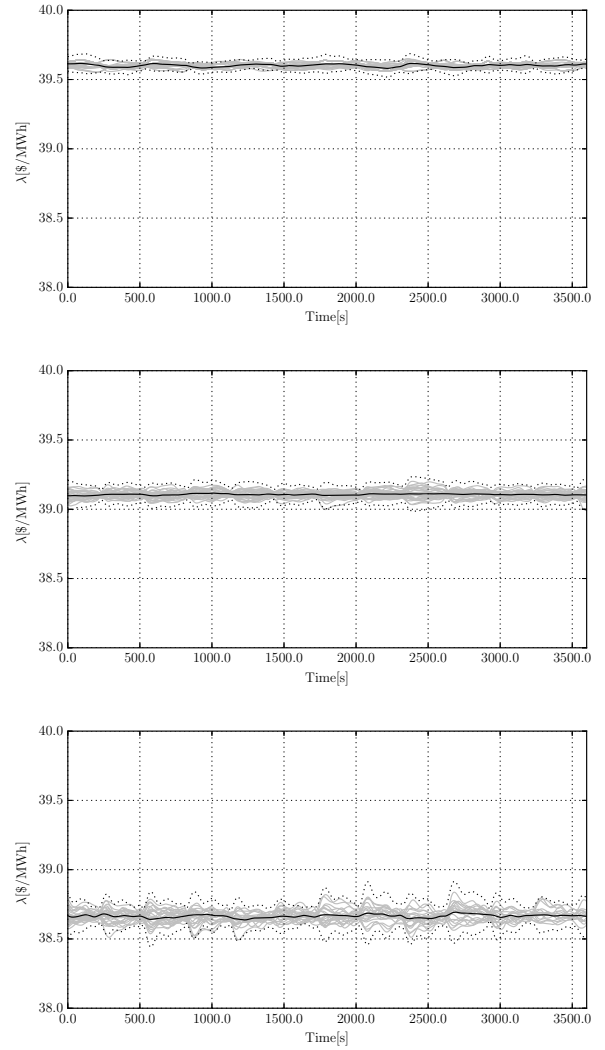

Fig. 5: Market clearing price λ with 2 (upper panel); 6 (middle panel); and 12 (lower panel) MGs. The grey lines represent each realization, the black thick line represents the average of the process, while the dotted line represents the average ± 3 times the standard deviation.
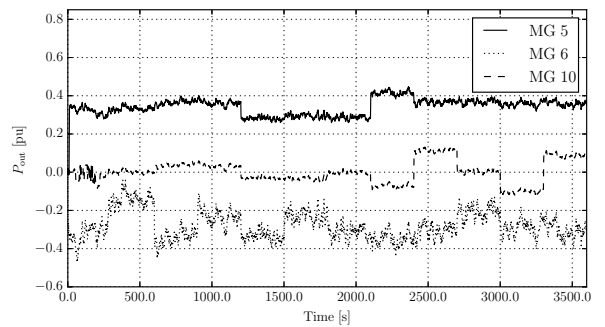

Fig. 6: Output powers P_{out} of three MGs.

B. DERs & Microgrids Scenario

This section discusses how differently MGs and DERs impact on system dynamics. With this aim, DERs are modeled assuming that they impose their active and reactive power productions P_g and Q_g, where P_g varies according to the

TABLE IV: DER parameters

DER	Bus	$\bar{P}_g$ (pu MW)	σ_g (pu MW)
1	18	0.88	0.013
2	3	0.77	0.040
3	15	0.80	0.020
4	17	0.40	0.040
5	21	0.20	0.020
6	28	0.20	0.020

TABLE V: Standard Deviation of the frequency of the COI as the number of DERs decreases and the number of MGs increases

# of DERs	# of MGs	σ_{COI} (pu Hz)
6	0	0.000951
3	3	0.000983
0	6	0.001121

TABLE VI: Standard deviation of the frequency of the COI as a function of the granularity k of MGs

k	# of MGs	σ_{COI} (pu Hz)
1	12	0.001788
2	24	0.003300
3	36	0.002390
4	48	0.001901
5	60	0.001654
6	72	0.001632
7	84	0.001624
8	96	0.001582
9	108	0.001546

stochastic process described in Section II. DERs are assumed not to provide frequency regulation.

Three configurations are considered in this subsection, as follows.

- 0 MGs, 6 DERs
- 3 MGs, 3 DERs
- 6 MGs, 0 DERs

To allow for a fair and consistent comparison of the behavior of MGs and DERs, the point of connections, the capacities as well as the mean and the standard deviation of active power set points of the DERs have same values as those used for the MGs in the previous subsection. Table IV shows the parameters for the considered DER units, while MG parameters are those of the first 6 rows of Table II. In Table IV, $\bar{P}_g$ and σ_g are, respectively, the average active power P_g produced by the DER during the simulation and its standard deviation.

Table V shows the standard deviation of ω_{COI} for the three considered configurations. Note that, to allow for a consistent comparison, the installed capacity of the DERs and MGs combined is 3.57 (pu MW) for all cases. Results indicate that the standard deviation of the frequency increases as the number of DERs decreases and the number of MGs increases. This is due to both load variations and active power set-point changes due to the EMSs of the MGs. It appears that, such a *greedy* behaviour, aimed to maximize MG profits, affects negatively the frequency standard deviation more than mere stochastic variations of uncontrolled DERs.

C. High Granularity of Microgrids Scenario

The results of the previous subsections suggest that, if the level of penetration of MGs and of unregulated DERs is increased, the deviation of the system frequency also consistently increases. The capacities considered in Subsections III-A and III-B are relatively high and can be assumed to represent large aggregated MG and DER models. Moreover, in the previous subsection, load and generator variations are strongly correlated for each MG, thus leading to relatively large steps of P_g and/or P_l for each MG.

This subsection studies the effect of the correlation of loads and generators within each MG. This is achieved by assuming different granularity levels, i.e., an increasing number of smaller MGs with uncorrelated powers connected at the same bus. With this aim, every each of the 12 MGs defined in Table II is split into k smaller MGs with capacity $1/k$ (see Table VI). For example, for $k = 4$, MG 1 is split into 4 MGs with $P_g = 0.22$, $P_l = 0.135$ and $\sigma = 0.00625$ (pu MW). Note that the total capacity of the MGs is 5.84 (pu MW) independently from the value of k. The random processes used to define the generation and the load of each MG are uncorrelated, i.e., fully independent from each other. Note that, to allow for a consistent comparison, the average generation and consumption levels are kept equal for each bus, independently from the granularity of the MG model.

Table VI shows that as k increases the standard deviation of ω_{COI} initially increases and then decreases. This is due to the averaging effect caused by the increasing number of independent random processes. This averaging effect is negligible below a certain number of units per bus (24 in this case). The standard deviation becomes smaller than the base-case ($k = 1$) only when the number of MGs reaches $k = 60$. Moreover, since the market clearing price λ depends on the frequency according to (4), a decrease of the standard deviation of ω_{COI} results in smaller oscillations of λ, and, in turn, each MG will adjust its active power set-point P_{ref} less frequently. It is thus reasonable to expect that as the granularity increases, the impact of MG EMS controllers on the transmission system dynamic response decreases. This is consistent with the assumption that MGs characterized by small capacities can be modeled as price takers.

D. Large Capacity Storage Microgrid Scenario

Subsection III-B shows that as the number of MGs increases with respect to the DER units, the standard deviation of the frequency of the COI increases. This fact suggests that the *greedy* behaviour of the MGs impacts on the frequency standard deviation more than the mere stochastic variations of uncontrolled DERs. To further investigate this aspect, this subsection compares the results obtained in Subsection III-A with MGs equipped with larger capacity storage.

Tables VII and VIII show, respectively, the new time constants for the MGs considered in the first scenario and the standard deviation of the frequency of the COI as the MG penetration level increases. For sake of comparison, the third column of Table III is included in Table VIII. Figures 7a and 7b compare the realizations of the frequency of the

TABLE VII: Large storage Microgrid parameters

MG	$\bar{P}_g$ (pu MW)	$\bar{P}_l$ (pu MW)	T_c (Hours)	σ_{net} (pu MW)
1	0.88	0.54	1.5	0.025
2	0.77	0.20	0.8	0.040
3	0.80	0.10	2.3	0.030
4	0.40	0.20	1.8	0.020
5	0.20	0.10	4.0	0.013
6	0.20	0.40	2.0	0.040
7	0.36	0.84	1.5	0.010
8	0.20	0.50	0.5	0.020
9	0.20	0.30	1.2	0.010
10	0.10	0.80	2.0	0.010
11	0.80	0.10	1.3	0.030
12	0.40	0.40	1.5	0.025

TABLE VIII: Standard deviation of the frequency COI as a function of the total MG installed capacity.

		Small storage	Large storage
Number of MGs	Capacity (pu MW)	σ_{COI} (pu Hz)	σ_{COI} (pu Hz)
1	0.96	0.000276	0.00082
2	1.81	0.000514	0.00124
3	2.69	0.000584	0.00135
4	3.13	0.000893	0.00188
5	3.35	0.000934	0.00194
6	3.57	0.001121	0.00210
7	3.97	0.001247	0.00243
8	4.19	0.001352	0.00269
9	4.41	0.001401	0.00292
10	4.52	0.001407	0.00339
11	5.40	0.001602	0.00414
12	5.84	0.001788	0.00496

COI, respectively, for the small capacity and the large capacity scenario.

Results show that the frequency standard deviation increases as the capacity of the storage gets larger. This increase is due to the fact that a large capacity storage increases the flexibility of the MG. If the storage capacity is small, the EMS is forced to buy/sell the deficit/surplus of energy of the MG as the storage device charges and discharges quickly. On the other hand, if the storage capacity is large, the EMS is able to take advantage of the electricity price, i.e., the EMS can sell or buy more power than it currently produces or needs, if the price is convenient. As it appears from simulations, greedy MGs equipped with large storage can impact negatively on the frequency of the COI.

IV. CONCLUSIONS

This paper proposes a stochastic framework to analyse the effects of the dynamic coupling of the transmission electrical system, the electricity market and the MGs. The proposed framework is utilized to define the impact of MGs on the transient response of the transmission systems and in particular, on its frequency; the different behavior of MGs and DERs; and the effect of MG correlation and granularity.

Simulation results show that the deviations of the frequency of the COI and, hence, the overall dynamic response of the transmission system, is consistently affected by the number, the size of MGs and by the dimensions of their storage units. Due to its *greedy* price-taker behavior, the bigger the size of

each MG and of its storage unit, the higher its impact on the system. In other words, a configuration with few large or several small but highly correlated MGs may not be feasible with the physical constraints of the electrical system. On the other hand, a high-granularity and uncorrelated configuration with several small MGs is likely more compatible with a proper operation of the system.

The fact that a high correlation of the response of several devices is detrimental to the stability of the overall system has been observed in other fields, such as traffic congestion, e.g., [29]. In control theory, this phenomenon is known as *flapping*. To mitigate such effect, it is possible to design stochastic distributed and/or decentralized controllers. Hence, future work will focus on the synthesis of appropriate controllers and/or the design of proper ancillary services to be provided by the microgrids to mitigate their negative impact on the system and, whenever possible, to leverage their penetration and improve the overall dynamic response of the transmission system.

REFERENCES

[1] H. Farhangi, *The Path of the Smart Grid*, IEEE Power and Energy Magazine, Vol. 8 , No. 1, pp. 18-28, 2010.
[2] R. H. Lasseter and P. Piagi, *Microgrid: A Conceptual Solution*, IEEE Power Electronics Specialists Conf., Vol. 6, pp. 4285-4290, 2004.
[3] S. Parhizi, H. Lotfi, A Khodaei and Shay Bahramirad, *State of the Art in Research on Microgrids: A Review*, IEEE Access, Vol. 3, pp. 890-925, 2015.
[4] N. Hatziargyriou, H. Asano, R. Iravani, and C. Marnay, *Microgrids: An Overview of Ongoing Research, Development, and Demonstration Projects*, IEEE Power Energy Magazine, pp. 78-94, 2007.
[5] A. Ulbig, T. S. Borsche, and G. Andersson, *Impact of Low Rotational Inertia on Power System Stability and Operation*, arXiv preprint arXiv:1312.6435, 2013.
[6] J. Zhang, S. Su, J. Chen, and F. Hong, *Stability Analysis of the Power System with the Large Penetration Ratios of Microgrids*, SUPERGEN, pp. 1-5, 2009.
[7] G. Lalor, A. Mullane, and M. O'Malley, *Frequency Control and Wind Turbine Technologies*, IEEE Trans. on Power Systems, Vol. 20, pp. 1905-1913, 2005.
[8] K. Folly and S. Sheetekela, *Impact of Fixed and Variable Speed Wind Generators on the Transient Stability of a Power System Network in Power Systems*, IEEE PSCE, pp. 1-7, 2009.
[9] H. Bevrani, *Robust Power System Frequency Control*, Springer, 2008.
[10] F. L. Alvarado, J. Meng , C. L. DeMarco , W. S. Mota, *Stability Analysis of Interconnected Power Systems Coupled with Market Dynamics*, IEEE Trans. on Power Systems, pp. 695-701, 2001.
[11] J. Nutaro and V. Protopopescu, *The Impact of Market Clearing Time and Price Signal Delay on the Stability of Electric Power Markets*, IEEE Trans. on Power Systems, Vol. 24, No. 3, 2009.
[12] Wei-Yu Chiu, H. Sun, and H. V. Poor, *A Multiobjective Approach to Multimicrogrid System Design*, IEEE Trans. on Smart Grid, Vol. 6, No. 5, pp. 2263-2272, 2015.
[13] Wei-Yu Chiu, H. Sun, and H. Vincent Poor, *Energy Imbalance Management Using a Robust Pricing Scheme*, IEEE Trans. on Smart Grid, Vol. 4, No. 2, pp. 896-904, 2013.
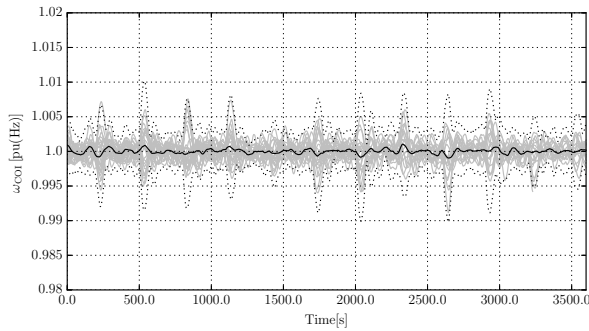
(a) Small storage capacity MG
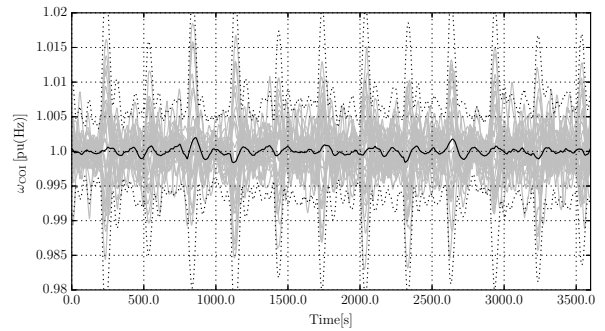
(b) Large storage capacity MG

Fig. 7: Frequency of the COI of the 39 bus system with 12 MGs. The grey lines represent each realization, the black thick line represents the average of the process, while the dotted line represents 3 times the standard deviation.

[14] J. P. Guerrero, J. C. Vásquez, J. Matas, L. García de Vicuna, M. Castilla, *Hierarchical Control of Droop-Controlled AC and DC Microgrids – A General Approach Toward Standardization*, IEEE Trans. on Industrial Electronics, Vol. 58, No. 1, pp. 158-172, 2010.

[15] Q. Shafiee, J. C. Vásquez, and J. M. Guerrero. *A Distributed Secondary Control for Islanded MicroGrids. A Networked Control Systems Approach*, IECON 2012 - 38th Annual Conference on IEEE Industrial Electronics Society, pp. 5637-5642, 2012.

[16] R. H. Lasseter, *Microgrid*, IEEE Power Engineering Society Winter Meeting, pp. 305-308, 2002.

[17] N. Pogaku, M. Prodanović and T. C. Green., *Modeling, Analysis and Testing of Autonomous Operation of an Inverter-Based Microgrid*, Power Electronics, IEEE Transactions, Vol. 22, pp. 613-625, 2007.

[18] E. H. M. Wittebol, A. Jokic and P. P. J. van den Bosch, *Dynamic Market Behavior of Autonomous Network based Power Systems*, Int. Conf. on Future Power Systems , 6 pp. -6, 2005.

[19] F. Milano, *Control and Stability of Future Transmission Networks*, in *The Handbook of Clean Energy Systems - Volume 4*, editor Prof. Jinyue Yan, John Wiley & Sons, June 2015.

[20] B. Tamimi, C. Cañizares and K. Bhattacharya, *Modeling and Performance Analysis of Large Solar Photo-Voltaic Generation on Voltage Stability and Inter-area Oscillations*, IEEE PES General Meeting, pp. 1-6, 2011.

[21] F. Milano and R. Zárate-Miñano, *A Systematic Method to Model Power Systems as Stochastic Differential Algebraic Equations*, in IEEE Trans. on Power Systems, vol. 28, no. 4, pp. 4537-4544, Nov. 2013.

[22] C. Roberts, E. M. Stewart, F. Milano, *Validation of the Ornstein-Uhlenbeck Process for Load Modeling Based on μPMU Measurements*, PSCC, Genoa, Italy, pp. 1-7, 2016.

[23] R. Palma-Behnke, C. Benavides, F. Lanas, B. Severino, L. Reyes, J. Llanos, D. Sáez, *A Microgrid Energy Management System Based on the Rolling Horizon Strategy*, IEEE Trans. on Smart Grid, vol. 4, no. 2, pp. 996-1006, June 2013.

[24] M. Mao, P. Jin, N. D. Hatziargyriou and L. Chang, *Multiagent-Based Hybrid Energy Management System for Microgrids*, IEEE Trans. on Sustainable Energy, vol. 5, no. 3, pp. 938-946, July 2014.

[25] W. Shi, X. Xie, C. C. Chu and R. Gadh, *Distributed Optimal Energy Management in Microgrids*, IEEE Trans. on Smart Grid, vol. 6, no. 3, pp. 1137-1146, May 2015.

[26] J. Xiao, P. Wang, L. Setyawan, *Implementation of Multiple-Slack-Terminal DC Microgrids for Smooth Transitions Between Grid-Tied and Islanded States*, IEEE Trans. on Smart Grid, vol. 7, no. 1, pp. 273-281, Jan. 2016.

[27] J. Xiao, P. Wang and L. Setyawan, *Multilevel Energy Management System for Hybridization of Energy Storages in DC Microgrids*, IEEE Trans. on Smart Grid, vol. 7, no. 2, pp. 847-856, March 2016.

[28] F. Milano, *A Python-based Software Tool for Power System Analysis*, in *Procs. of the IEEE PES General Meeting*, Vancouver, BC, July 2013.

[29] A. Schlote, C. King, E. Crisostomi, R. Shorten, *Delay-tolerant stochastic algorithms for parking space assignment*, IEEE Trans. on Intelligent Transportation Systems, vol. 15, no. 5, pp. 1922-1935, 2014.
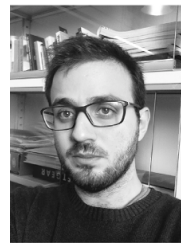
Pietro Ferraro received the M.Sc. degree in automatics and robotics from the University of Pisa, Italy, in 2014. He is currently a Ph.D. candidate with the Department of Energy, Systems, Territory and Constructions Engineering, University of Pisa. His research interests include control theory, optimization and time series analysis, with application to smart grids.

Emanuele Crisostomi received the B.Sc. degree in computer science engineering, the M.Sc. degree in automatic control, and the Ph.D. degree in automatics, robotics, and bioengineering, from the Univ. of Pisa, Italy, in 2002, 2005, and 2009, respectively. He is currently an Assistant Professor of electrical engineering with the Department of Energy, Systems, Territory and Constructions Engineering, Univ. of Pisa. His research interests include control and optimization of large scale systems, with applications to smart grids and green mobility networks.

Marco Raugi received the Ph.D. degree in electrical engineering from the University of Pisa, Pisa, Italy, in 1990. Currently, he is a Full Professor of Electrical Engineering with the Department of Energy, Systems, Territory and Constructions Engineering, University of Pisa. He is the author of many papers in international journals and conference proceedings. His research interests include numerical electromagnetics, with main applications in nondestructive testing, electromagnetic compatibility, communications, and computational intelligence. Prof. Raugi was the General Chairman of the international conferences Progress in Electromagnetic Research Symposium in 2004 and IEEE International Symposium on Power Line Communications in 2007. He was the recipient of the IEEE Industry Application Society 2002 Melcher Prize Paper Award.

Federico Milano (S'02, M'04, SM'09, F'16) received from the Univ. of Genoa, Italy, the ME and Ph.D. in Electrical Eng. in 1999 and 2003, respectively. From 2001 to 2002 he was with the Univ. of Waterloo, Canada, as a Visiting Scholar. From 2003 to 2013, he was with the Univ. of Castilla-La Mancha, Spain. In 2013, he joined the Univ. College Dublin, Ireland, where he is currently Professor of Power Systems Control and Protections. His research interests include power system modeling, control and stability analysis.